BEHAVIOUR OF PRESSURE SENSORS UNDER THE INFLUENCE OF IONIZING AND NON-IONIZING RADIATION

ESTORIL, PORTUGAL | 09 – 13 MAY 2022

Kyra Bekaan [(1)], Heiko Dartsch [(2)], Anastasios Stomas [(3)], Hans-Peter Harmann [(4)]

[(1)] AST Advanced Space Technologies, Osterholz-Scharmbeck, Germany, Email: kyra.bekaan@ast-space.com
[(2)] AST Advanced Space Technologies, Osterholz-Scharmbeck, Germany, Email: dartsch@ast-space.com
[(3)] STS Sensor Technik Sirnach AG, Sirnach, Switzerland, Email: entwicklung@stssensors.com
[(4)] AST Advanced Space Technologies, Osterholz-Scharmbeck, Germany, Email: harmann@ast-space.com

KEYWORDS: Pressure sensors, ionizing radiation, non-ionizing radiation, radiation hardening

ABSTRACT:

AST (ADVANCED SPACE TECHNOLOGIES GMBH) HAS INVESTIGATED THE INFLUENCE OF IONIZING AND NON-IONIZING RADIATION ON THE TYPE OF PRESSURE SENSOR CELLS USED IN THEIR PRODUCTS. THE INTEND WAS TO CONFIRM HIGH RELIABILITY AND TO IMPROVE LONG-TERM OPERATION PRESSURE READING ACCURACY FOR OPERATION IN HIGH RADIATION SPACE ENVIRONMENT.

A COMPLEX TEST SETUP ALLOWED TO PRESSURIZE THE SENSORS CYCLICALLY TO DIFFERENT PRESSURE LEVELS DURING THE EXPOSURE TO RADIATION LOADS.

WE WILL PRESENT THE DETAILS OF OUR TEST SETUP, DEMONSTRATING A MODEL DERIVED FROM THE TEST DATA, WITH WHICH THE MEASUREMENT ACCURACY OF THE PRESSURE SENSORS CAN BE PREDICTED BY MEANS OF THE DOSE RECEIVED DURING THE MISSION. FURTHERMORE, WE WILL SHOW THAT THE RADIATION HAS NO SIGNIFICANT EFFECT ON RELIABILITY OF THE PRESSURE SENSORS.

AT CERTAIN DOSE LEVELS, RADIATION INDUCED DRIFT EFFECTS STARTED TO SHOW SATURATION, OPENING UP THE POSSIBILITY OF PRE-IRRADIATING SENSORS TO MINIMIZE DRIFT EFFECTS.

1. INTRODUCTION

In any space mission, whether LEO (Low Earth Orbit), MEO (Medium Earth Orbit), GEO (Geostationary Orbit) or deep space, background radiation from space is a major factor that must be considered. In general, electrical components are sensitive to ionizing radiation. Sensor components can suffer from a significant loss in accuracy induced by radiation exposure.
Due to the Van Allan radiation belts and the protons and electrons trapped in them, radiation is relatively high in these areas, as can also be seen in Fig. 1. The maximum annual dose with 4mm Aluminium shielding is approximately 5 krad. Especially for components installed outside the spacecraft, the components are covered by much less shielding. Fig. 2 shows that the dose decreases strongly with increasing shielding. It can be concluded that outside the spacecraft, doses of several 100 krad up to the Mrad range can be achieved.

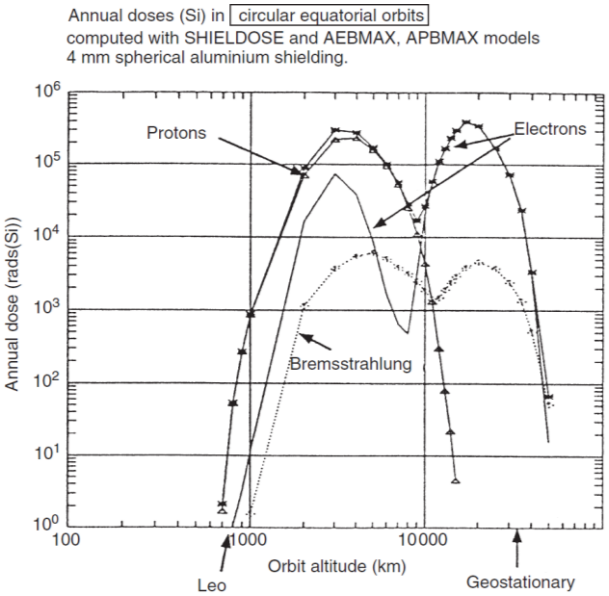

Figure 1: Annual radiation with 4mm spherical aluminium shieling in dependence of orbit altitude [1]

For a typical mission with AST's products (10 years in LEO orbit), a dose of up to 40 krad can be assumed considering its intrinsic shielding.
The most radiation-sensitive components of the AST products are the pressure sensors. The existing studies on the behaviour of pressure sensors under the influence of radiation have a relatively low resolution and were performed only at one pressure level.
Therefore, AST decided to conduct elaborate test campaigns investigating the influence of ionizing

radiation on pressure sensors. During the tests, the pressure sensors were regularly pressurized with different pressure levels and continuously read out so that the change over increasing radiation dose can be analysed. A similar test regarding non-ionizing radiation was performed with neutrons.

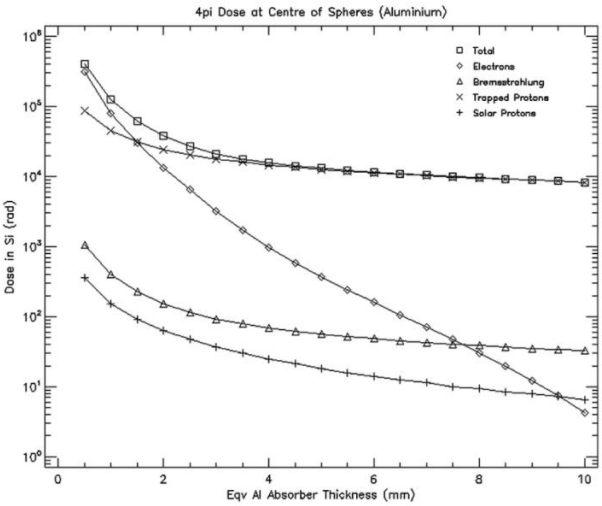

Figure 2: Dose in dependence of the aluminium equivalent shielding [2]

2. TEST FACILITIES

The irradiation took place at the "Fraunhofer-Institut für Naturwissenschaftlich-Technische Trend-analysen INT" in Euskirchen, Germany, using a ^{60}Co source with a maximum dose rate of 720 krad/h and a separate neutron source.
The isotope ^{60}Co decays with a half-life of about 5.3 years by beta decay to ^{60}Ni, which decays to the ground state of nickel by emitting gamma radiation of energies 1.172 MeV and 1.332 MeV [3].
The THERMO-Fisher D-711 neutron generators at Fraunhofer INT produce neutrons by accelerating deuterium ions (D = 2H) with a voltage of 150 kV onto deuterium or tritium targets (T = 3H). Within the target, D-D or D-T nuclear fusion reactions take place, releasing helium isotopes 3He and 4He, respectively, and fast neutrons with energies of 2.5 MeV and 14.1 MeV, respectively [4].

3. DEVICE UNDER TEST

Two types of pressure sensors with a full range reading of 4 bar and 350 bar were tested. Both types have the same design and technology, they differ only in the sensitivity of the sensing element.
AST uses the very same types of sensors in their products, as can be seen in Fig. 3.
The sensing elements are passive bridge type sensors, the circuit diagram of the sensors is shown in Fig. 4. The sensor cells do not contain any active electronics which means that enhanced low dose rate sensitivity (ELDRS) does not have to be considered.

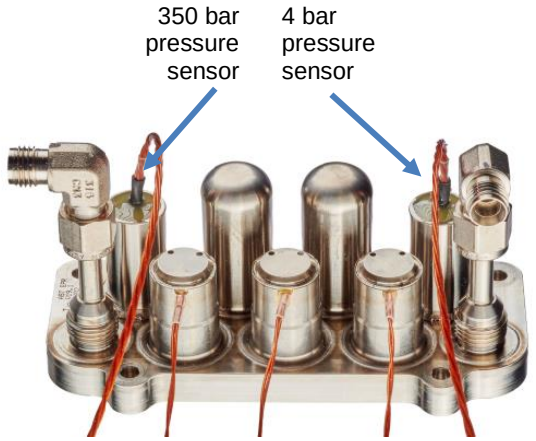

Figure 3: EPR (Electronic Pressure Regulator) from AST. One example of AST's use of the pressure sensor. The pressure sensors are marked with an arrow.

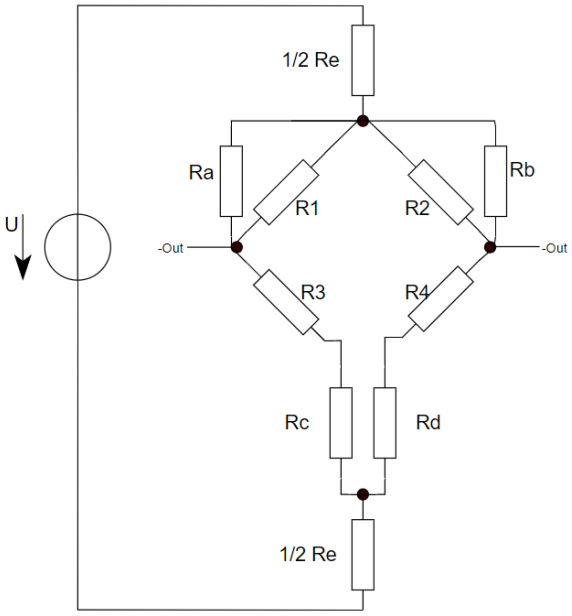

Figure 4: Circuit diagram of a pressure sensor (voltage supply)

As can be seen, the sensor circuit consists of a Wheatstone bridge (R1 – R4) and additional resistors connected in series or parallel (Ra – Re). The additional resistors are used to reduce the initial sensor offset as well as the temperature dependant drift of sensor sensitivity and offset. During manufacturing, for each individual sensor cell the corresponding resistance values are determined by high-precision measurements over pressure and temperature. The fixed value resistors (Ra – Re) used are surface mounted thick film resistors. This resistor technology is known to be insensitive to radiation which was also confirmed by a dedicated test conducted in the frame of the performed irradiation campaign for a TID (Total Ionizing Dose) of up to 40 Mrad.

4. TEST DESCRIPTION

Throughout the tests, the sensors are operated continuously by supplying them with nominal current. During this process, measurements are carried out at different pressure levels. To be able to read the sensors continuously during the irradiation time, each sensor is electrically connected. In addition, each sensor is equipped with a fluidic connection so that each sensor can be cyclically pressurized during the entire irradiation time. A distinction is made between the 4 bar and 350 bar sensor cells so that different pressure levels can be achieved. This allows a high temporal resolution of the measurement data over the complete dose.

In case of gamma radiation from ^{60}Co decay the intrinsic shielding resulting from the sensor housing made from stainless-steel corresponds to an attenuation factor of 0.88 [5]. In the following, a worst-case attenuation factor of 80% is assumed.

The sensors are supplied with the nominal current and the voltage and current were measured in situ to calculate the resulting resistances R1 - R4.

During irradiation, the sensors were cyclically pressurised to four different pressure levels with nitrogen and the resulting individual resistance values R1, R2, R3 and R4 were recorded. The sensor output signal U_e was calculated from the measured resistance values and the values for the additional fixed-value resistors as determined during sensor manufacturing. U_e corresponds to the differential voltage between out+ and out- in Fig. 4. In this way U_e is calculated for all four pressure levels applied. The voltage and the pressure show a highly linear relation and can thus be described by a linear approximation (y = m*x+b) with a certain sensitivity *m* and a certain offset *b*.

In all tests, before the radiation source was activated, a period of time was measured without radiation in order to obtain a zero line that can be referred to in later measurements.

The respective data is shown as relative data in each case. This means that the data is based on the mean value before the irradiation. Thus, the relative deviation can be read on the y-axis. The offset is always calculated on the full-scale value, so a value of 4 bar is assumed for the 4 bar sensor. Although the full scale (FS) for the second sensor is 350 bar, only a full scale value of 180 bar is assumed, as this is used in most of AST's current applications. A lower full scale value results in a higher percentage deviation for the offset.

5. TESTS WITH IONIZING RADIATION

Two irradiation test runs were performed with ionizing radiation. In the first test, the sensors were irradiated up to a TID of 8 Mrad. In a second test at lower dose rate and therefore higher temporal resolution, irradiation was performed up to a TID of 240 krad. The values refer to the actual dose at the sensor's sensing element, so shielding has already been considered.

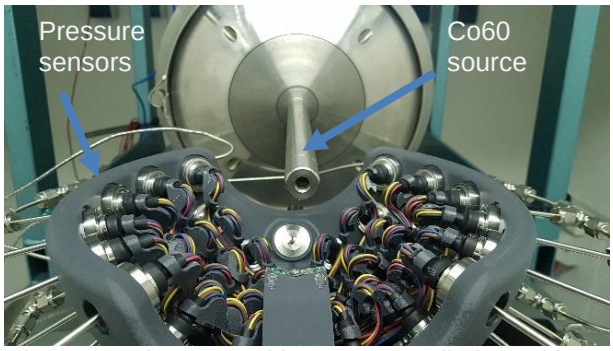

Figure 5: First test with gamma radiation with 42 individual sensors irradiated up to a TID of 8 Mrad

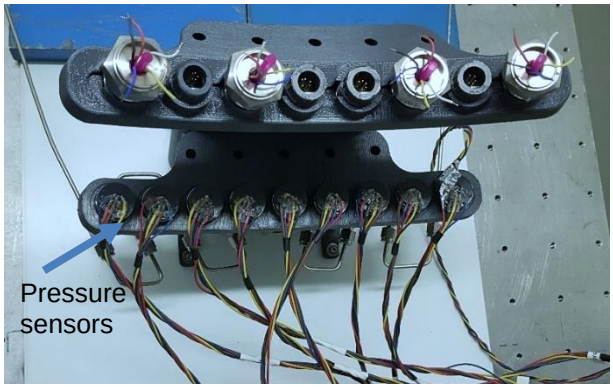

Figure 6: Second test with gamma radiation with 9 sensors irradiated up to a TID of 240 krad

Typical values for the TID in space missions for AST's products are between 5 - 50 krad, which is why the focus is placed on the evaluation of the second test, in which to a TID of 240 krad was irradiated.

The first test, in which the pressure sensors were irradiated with a dose of 8 Mrad, not one of the 42 tested sensors failed or showed unexpected behaviour.

The data from the tests were evaluated and analysed in detail. The four installed resistors in the form of strain gauges show a change in value with increasing radiation, due to the physical change of the installed sensing element of the sensor. Depending on the applied pressure, the individual values of the resistors differ more or less from each other, but each resistor of each sensor shows the same effects when irradiated, which is reflected in the sensitivity and offset. Fig. 7 shows all sensors of the first test. As can be seen, the change in sensitivity and offset of the different sensors differ slightly but show a consistent behaviour.

To make the figures clearer, only the results of a single sensor are shown in each case, and only the change of the resistance of one resistor of one sensor is shown when evaluating the individual resistors.

Fig. 8 shows the result of the data regarding one individual bridge resistor of one 4 bar sensor. The black dashed line indicates the start of the

irradiation. To the left side of the dashed line the TID is plotted over time (upper x-axis), to the right it is plotted against TID (lower x-axis). The y-axis shows the corresponding relative change in resistance.

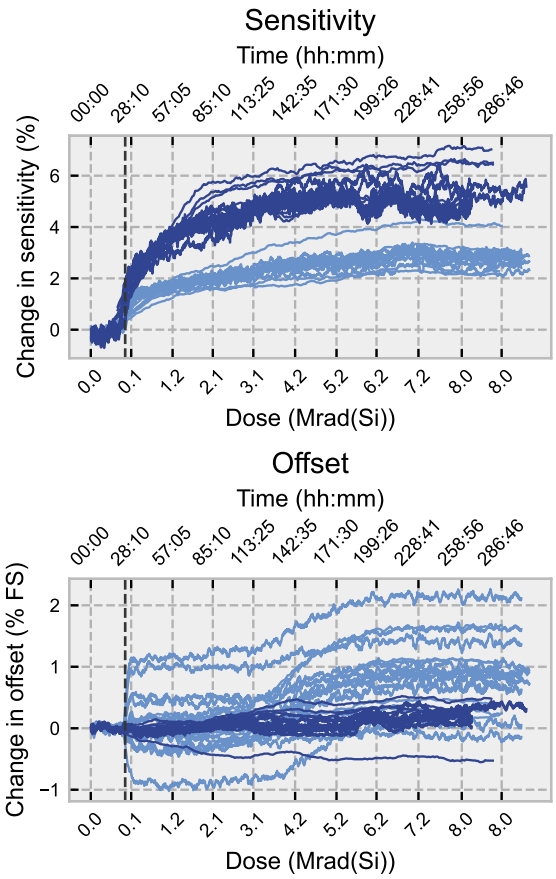

Figure 7: Change in sensitivity and offset of all irradiated pressure sensors from the first test run. The light blue lines represent the 4 bar sensors and the dark blue lines the 350 bar sensors.

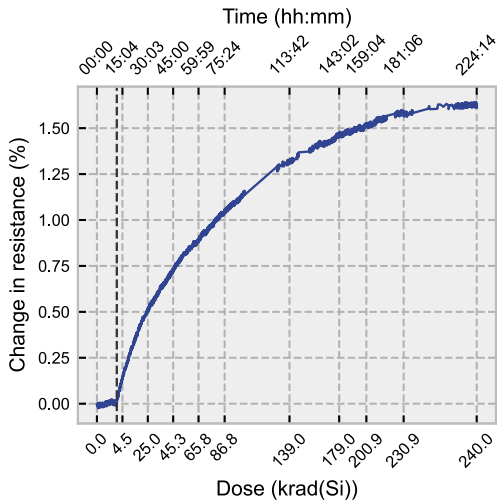

Figure 8: Change of resistance of one installed resistor on one 4 bar pressure sensor over the TID of 240 krad.

The individual resistances increase by about 1.7 % over the complete dose of 240 krad. A saturation effect is observed, therefore, at the beginning of the irradiation, the change is clearly more pronounced.

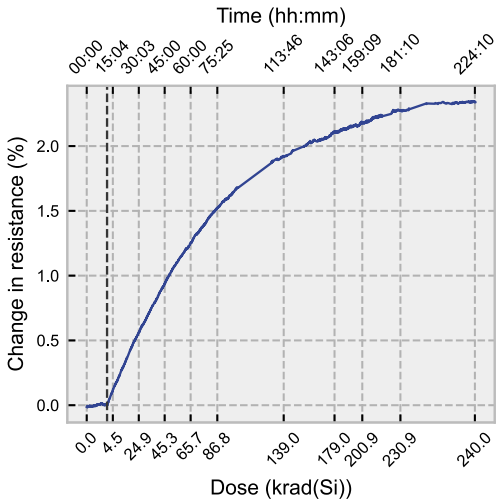

Figure 9: Change of resistance of one installed resistor on one 350 bar pressure sensor over the TID of 240 krad.

The 350 bar sensor shows similar behaviour, but the maximum relative change in resistance after a TID of 240 krad is significantly higher than the 4 bar sensor with about 2.4% change, as can be seen in Fig. 9. Up to a TID of about 25 krad the relative change of the two sensor types is similar, but saturation starts later for the 350 bar sensor.

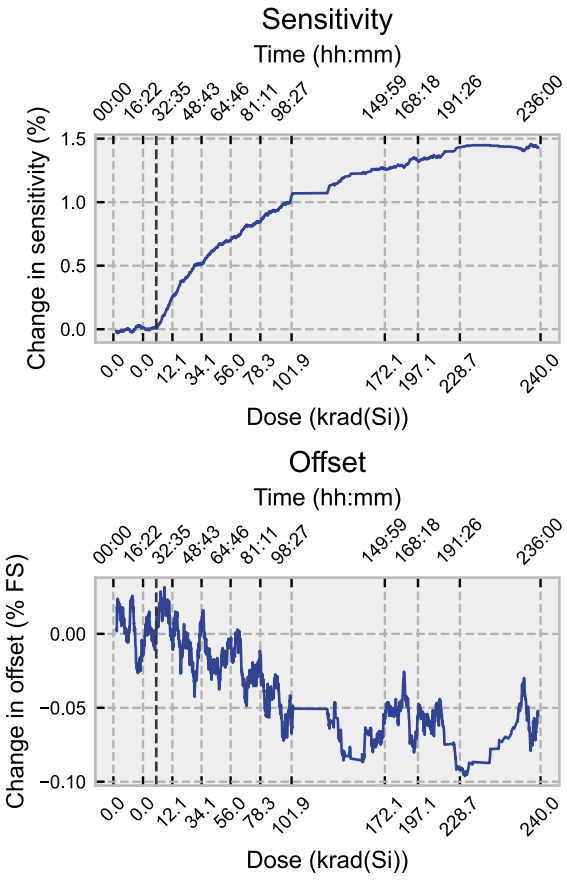

Figure 10: Change of sensitivity and offset of one 4 bar sensor over the TID of 240 krad.

Fig. 10 shows the change in sensitivity and offset from one irradiated 4 bar sensor over the TID as derived by calculation using the measured bridge resistance values, as well as the values for the fixed value resistors specific for this individual sensor cell. Here, too, the black dashed line shows the start of irradiation and the calculated sensitivity increases with increasing radiation, where again a saturation effect can be observed. In the lower graph, it can be observed that the change in offset decreases slightly compared to the values before irradiation.
Fig. 11 shows the processed data for the 350 bar sensor.
The behaviour of the 350 bar sensor is very similar to that of the 4 bar sensor in terms of sensitivity. The same saturation effect is observed, so at the beginning the change in sensitivity increases faster. Moreover, the maximum change in sensitivity in correlation with the change in bridge resistances is also higher. With a TID of 240 krad, the sensitivity changes by more than 2.5%. The offset increases here in contrast to the 4 bar sensor with increasing TID. The increase is nearly linear, but from 230 krad a plateau can be observed.

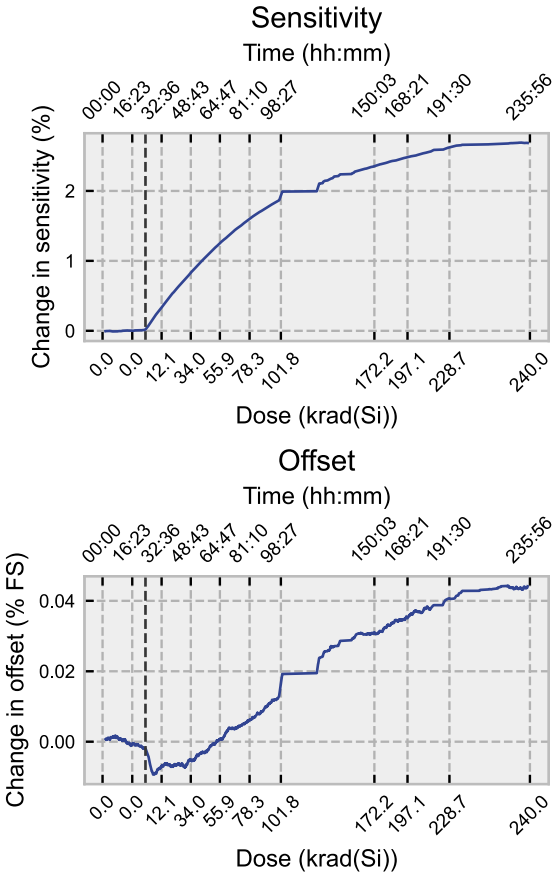

Figure 11: Change of sensitivity and offset of one 350 bar sensor over the TID of 240 krad.

6. RADIATION HARDENING

In the first irradiation test, in which the pressure sensors were exposed to a dose of 8 Mrad, a saturation effect was observed for sensitivity and offset. This fact suggest that it is possible to "harden" the sensors with respect to radiation induced effects, i.e., that the sensors, when they have already experienced a certain dose, show no or at least fewer changes.
Therefore, some sensors from the first test were reused for the second test. In total, there were three sensors that had already been exposed to a TID of 8 Mrad before they were irradiated again with a TID of 240 krad.
Fig. 12 shows an excerpt of the evaluation of the pre-irradiated 4 bar sensors. The relative change of a single resistor installed on one pressure sensor is shown. For better comparability, the values from the previous chapter, i.e., the non-pre-irradiated sensors, are also shown in dark blue. These are two different sensors of the same type. The pre-irradiated sensors from the first test are drawn in light blue.

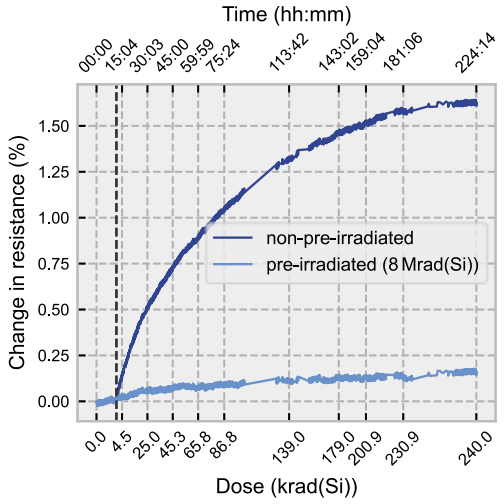

Figure 12: Change in resistance of one individual bridge resistors of a pre-irradiated 4 bar sensor in comparison to a 4 bar sensor without pre-irradiation.

As can be seen, the individual resistances only increase by about 0.2% over the complete TID of 240 krad, which is only about 12% of the change without pre-irradiation.
Although the change of the individual resistors was significantly higher for the 350 bar sensors than for the 4 bar sensors (2.4% instead of 1.7%), the change can also be reduced to about 0.2% by pre-irradiation. In this case, this corresponds to only about 8% of the original value. The results can be seen in Fig. 13.
Fig. 14 shows the deviations in sensitivity and offset of one 4 bar sensor. The results from the previous chapter are also shown here in dark blue, the pre-irradiated sensors in light blue.
The difference in sensitivity is very clear: While the sensitivity of the non-pre-irradiated sensors changes by about 1.4% over the entire irradiation period, the pre-irradiated sensors only change by about 0.15%, i.e., by only one tenth of the originally achieved value.

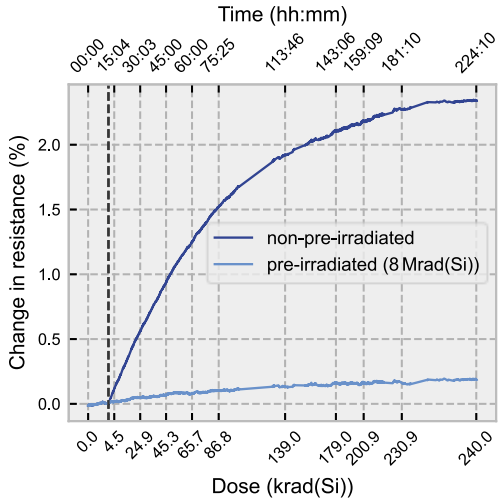

Figure 13: Change in resistance of one individual bridge resistors of a pre-irradiated 350 bar sensor in comparison to a 350 bar sensor without pre-irradiation.

The effect of radiation hardening is different with offset: While non-pre-irradiated 4 bar sensors drift into the negative range (max. -0.12% FS), the offset of pre-irradiated sensors drifts into the positive range (max. +0.15% FS). The offset error, viewed in absolute values, is therefore approximately the same in both cases.

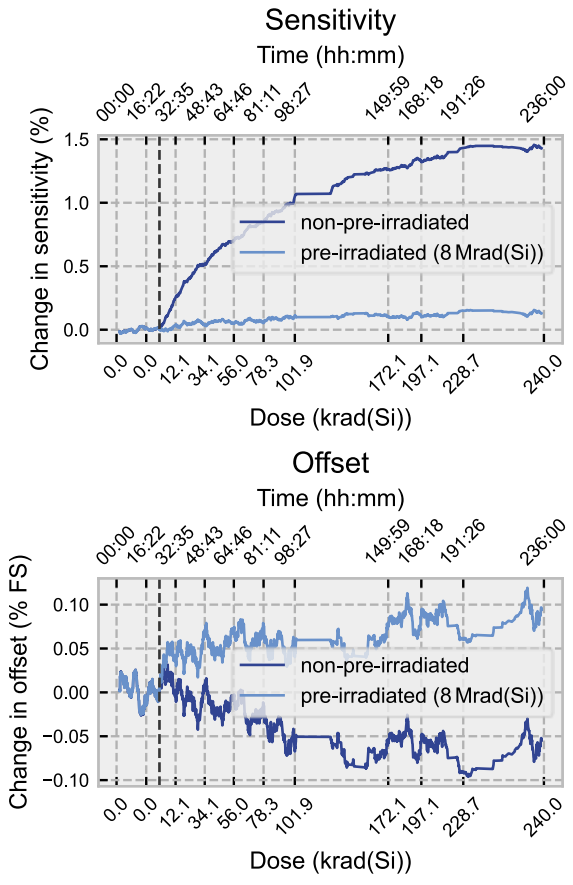

Figure 14: Change in sensitivity and offset of one 4 bar Sensor up to a dose of 240 krad in comparison to one non-pre-irradiated 4 bar sensor.

The following Fig. 15 shows the evaluation of a 350 bar sensor.
For the sensitivity of the 350 bar sensor, a similar behaviour can be observed for the pre-irradiated sensors. The sensitivity of the pre-irradiated sensors changes only by about 0.3% at a TID of 240 krad, instead of 2.7% as for the non-pre-irradiated sensors, so a reduction of almost 90% can be observed.
The change in offset is not very high, even for the non-pre-irradiated 350 bar sensors, at 0.04%, but can be reduced by more than half to about 0.02% by pre-irradiation.

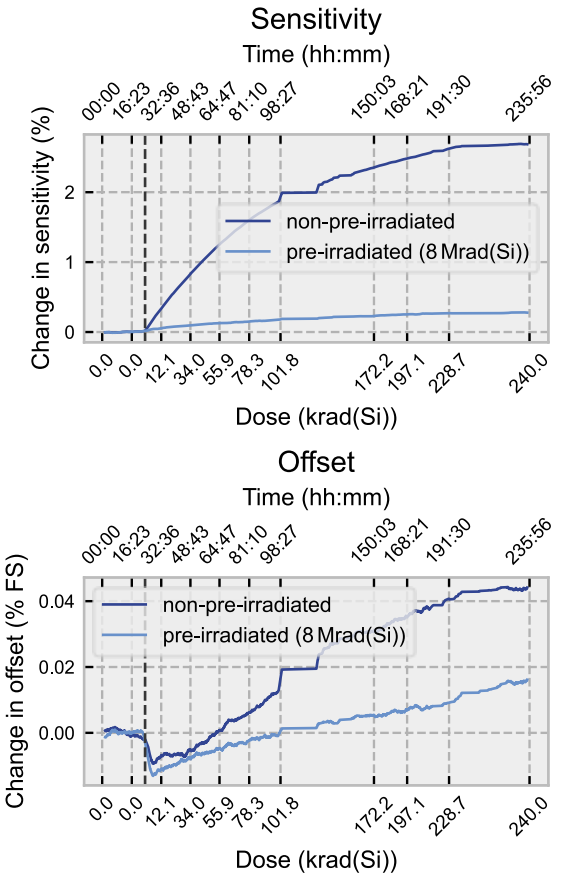

Figure 15: Change in sensitivity and offset of one 350 bar Sensor up to a dose of 240 krad in comparison to one non-pre-irradiated 350 bar sensor

7. TESTS WITH NON-IONIZING RADIATION

During the neutron irradiation, a total non-ionizing dose of $1*10^9$ MeV/g(Si) was reached, which is equivalent to $2.6*10^{11}$ neutrons@14 MeV/cm^2.
The dose applied covers the typical applications of AST's products. This test also showed that there were no sensor failures over the entire test period, just as in the tests with gamma radiation. The impact of radiation induced effects on the overall reliability of a pressure sensor is therefore neglectable.

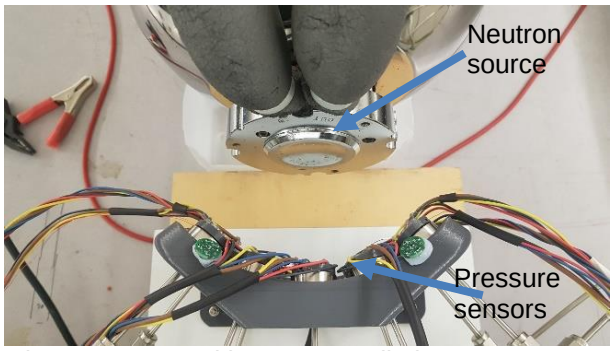

*Figure 16: Test with neutron radiation up to a TNID of 1*10^9 MeV/g(Si) with nine pressure sensors.*

Fig. 17 and Fig. 18 show the change of one resistor value installed on one pressure sensor during irradiation with neutrons.

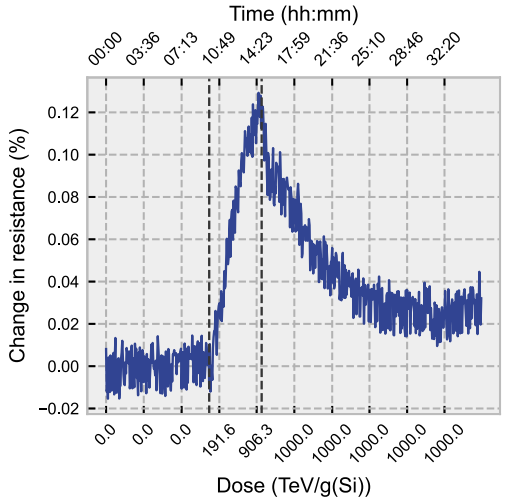

Figure 17: Change in resistance of one individual bridge resistor of one 4 bar sensor.

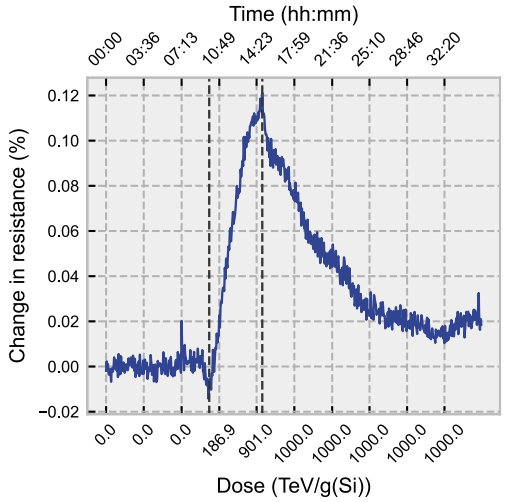

Figure 18: Change in resistance of one individual bridge resistor of one 350 bar sensor.

The change in resistance rises as long as the radiation source is activated. But in contrast to gamma irradiation, the change in resistance is partially revisable. In the case of the 4 bar sensor, after a TNID of 1*10^9 MeV/g(Si), the change in resistance is 0.13%, but this decreases after some time to below 0.025%. For the 350 bar sensor, a value of 0.12% is reached after the TNID (Total Non-Ionizing Dose), which reduces to about 0.02% after irradiation due to the self-annealing after the end of the irradiation.

In this test, a very high dose rate was used, so a TNID which covers a majority of mission scenarios was applied in a short time (1*10^9 MeV/g(Si) in 5 hours), instead of over several years as under real conditions. It can therefore be assumed that under real conditions the healing effect, which are now only visible after the end of irradiation, occur earlier and the deviation of the values is not so high. However, the the change in resistance of 0.13% and 0.12% can be taken as a worst-case estimate for a TNID of 1*10^9 MeV/g(Si).

Fig. 19 shows the change in sensitivity and offset of a 4 bar sensor.. The sensitivity increases during irradiation in correlation to the individual resistances up to about 0.06%. The offset does not change during the irradiation. Since small values increase the relative change and therefore the uncertainty, these values should be considered with caution.

The change in sensitivity decreases to about 0.02% after the end of the irradiation with some uncertainty due to noise.

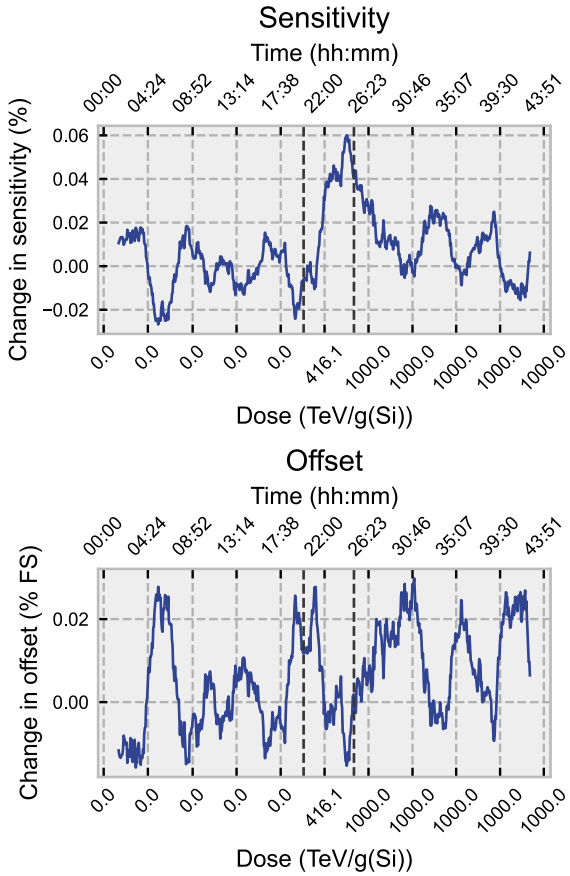

*Figure 19: Change in sensitivity and offset of one 4 bar sensor over a TNID of 1*10^9 MeV/g(Si).*

Fig. 20 shows the change in sensitivity and offset for the 350 bar sensor. The change in sensitivity

increases by about 0.04% during irradiation. After the end of the irradiation, this value drops to 0.01%. Up to the maximum TNID, the change in offset decreases to a value of -0.007%, as soon as the irradiation is stopped, the value stops decreasing and remains constant.
As mentioned before, the effect is overpronounced due to high dose rate which is not representative for real conditions. Hence, the results can be regarded as worst-case estimations.

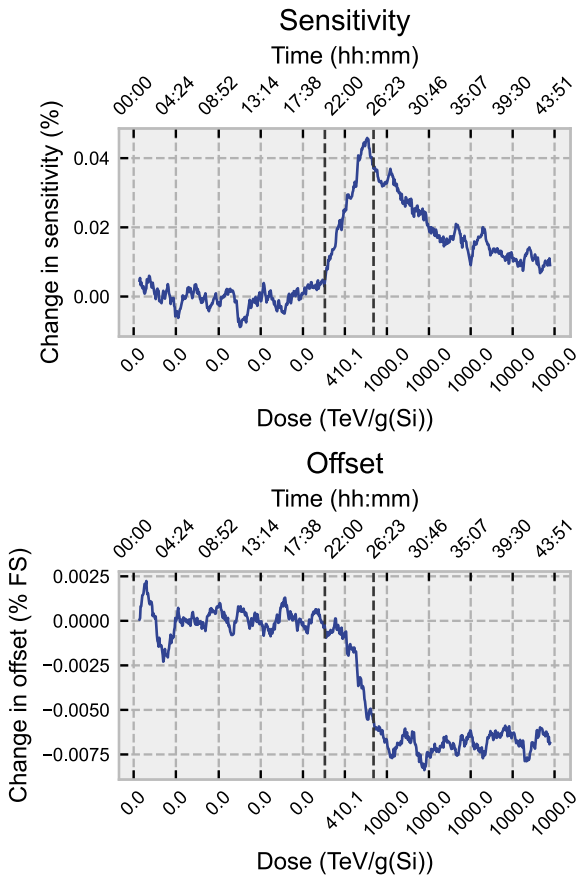

*Figure 20: Change in sensitivity and offset of one 350 bar sensor over a TNID of 1*10⁹ MeV/g(Si).*

8. SUMMARY AND CONCLUSION

In summary, it has been shown that the pressure sensors are sensitive to gamma radiation but can still withstand a very large dose of radiation (8 Mrad) and shows no signs of failure. The impact of radiation induced effects on the overall reliability of a pressure sensor is therefore neglectable.
Based on these measurements, AST now has an empirical model of the effects of ionizing and non-ionizing radiation on the performance of the pressure sensors and can therefore predict the end-of-life performance of AST's products for any given mission environment.
For example, this results in a maximum contribution to end-of-life error for the 4 bar pressure sensor of < ± 0.5% for an AST product in a typical LEO mission, caused by radiation effects. For the 350 bar sensor, this results in a value of < ± 0.8%.

The sensitivity to gamma radiation can be reduced if the sensors are pre-irradiated, this reduces the relative chance in sensitivity to about 1/10 of the change in sensitivity with a non-pre-irradiated pressure sensor at the same TID.
In case of irradiation with non-ionizing radiation, a small increase in sensitivity and offset can be observed, but this evens out after the end of irradiation.
The observed self-annealing shows that the effect of irradiation is overemphasized due to the high dose rate and the resulting error is actually lower, so the change in sensitivity and offset obtained in the tests with neutrons can be taken as worst-case estimations.

9. ACKNOWLEDGEMENTS

This research was funded by the 2020 Horizon projects CHEOPS (Grant Agreement Number: 730135, https://www.cheops-h2020.eu/) and GIESEPP (Grant Agreement Number: 730002, https://www.giesepp.com/). AST likes to thank the Fraunhofer INT in Euskirchen for their support.

10. REFERENCES

1. Fortescue, P., Swinerd, G., & Stark, J. (Eds.). (2011). *Spacecraft Systems Engineering* (4th ed.). Wiley.

2. Neubert, T., Rongen, H., Froehlich, D., Schardt, G., Dick, M., Nysten, T., Zimmermann, E., Kaufmann, M., Olschewski, F., & van Waasen, S. (2019). System-on-module-based long-life electronics for remote sensing imaging with CubeSats in low-earth-orbits. *Journal of Applied Remote Sensing*, *13*(03), 1. https://doi.org/10.1117/1.jrs.13.032507

3. Fraunhofer INT. (2022a). Cobalt-60 Bestrahlungsanlagen. Retrieved March 28, 2022, from https://www.int.fraunhofer.de/de/geschaeftsfelder/nukleare_effekteinelektronikundoptik/bestrahlungsanlagen/neutron-generator-.html

4. Fraunhofer INT. (2022b). Neutronengenerator. Retrieved March 28, 2022, from https://www.int.fraunhofer.de/de/geschaeftsfelder/nukleare_effekteinelektronikundoptik/bestrahlungsanlagen/neutron-generator-.html

5. Half-Value Layer. (n.d.). Nondestructive Evaluation Physics: X-Ray. Retrieved March 16, 2022, from https://www.nde-ed.org/Physics/X-Ray/HalfValueLayer.xhtml